Influence of Composite Coating (Tin/BN) On Microstructure and Properties of Laser-Cladded Martensitic Stainless-Steel Coating

ISSN: 2073-9524

Pages:57-66

Mariam Ahmed ¹*, Al katawy Ali adwan ¹, Abeer A.Shehab ¹

¹ Department of Materials Engineering, College of Engineering, Diyala University, Diyala, 32001, Iraq eng_grad_materials4@uodiyala.edu.iq, dr.ali_edwin@uodiyala.edu.iq, abeer_shihab_eng@uodiyala.edu.iq

Abstract

The current work used the laser cladding method to prepare a composite coating of titanium nitride (TiN) combined with boron nitride (BN) on 420 stainless steels. The microstructure, micro-hardness, wear resistance, and bio-corrosion resistance of the coatings were analyzed using scanning electron microscopy (SEM), energy-dispersive spectroscopy (EDS), a micro-hardness tester, a wear tester, a bio-corrosion resistance test, and electrochemical techniques. The results indicated that a strong metallurgical bond was successfully formed between the composite coating and the substrate. SEM analysis revealed that the sample produced at low power demonstrated superior performance compared to the high-power sample with respect to the microstructure. The path coefficients related to adhesion factors, such as microhardness, were higher in the low-power sample, suggesting stronger and more consistent interactions between the coating and the substrate. EDS results showed that the high-power sample had a lower iron (Fe) signal, indicating superior performance in that regard; however, the low-power sample displayed strong titanium (Ti) and BN components. Micro-hardness decreased with high power and increased with low power. The high-power sample exhibited a higher wear rate compared to the low-power counterpart. In the bio-corrosion test, the uncoated martensitic steel displayed a more negative and unstable open circuit potential (OCP) profile. In contrast, the TiN + BN-coated sample showed a less negative and more stable OCP response, indicating enhanced corrosion resistance. Electrochemical techniques demonstrated that the "Mix" sample had superior electrochemical performance compared to the "Base" sample. It exhibited a broader current density range, a higher current response, and clearer separation of anodic and cathodic reactions, making it more effective for applications in medical instruments such as orthopedic implants, dental implants (abutments and dental screws), surgical tools (scalpels, forceps, bone drills), and spinal implants and plates. Electrochemical techniques demonstrated that the "Mix" sample had superior electrochemical performance compared to the "Base" sample. It exhibited a broader current density range, a higher current response, and clearer separation of anodic and cathodic reactions, making it more effective for applications in medical instruments.

Keywords: Laser Cladding, Martensitic Stainless Steel, Titanium Nitride, Boron Nitride.

Article history: Received: 29 May 2025, Accepted: 30 Aug 2025, Published: 15 Sep 2025.

This article is open-access under the CC BY 4.0 license (http://creativecommons.org/licenses/by/4.0/).

^{*} Corresponding author: eng grad materials4@uodiyala.edu.iq

1. Introduction

Laser cladding generates a metallurgical bond between the coated layer and substrate, while producing a narrower heat affected zone with a finer grain size compared to arc welding. Moreover, it is known for its low dilution rate, rapid thermal cycle, minimal thermal distortion, excellent metallurgical properties and the formation of supersaturated solid solutions [1]. Martensitic stainless steels (MSS) are regarded as highly suitable materials for laser cladding due to their low cost and favorable mechanical properties [2]. It is regarded as a promising alloy for additive manufacturing of functional coatings and components due to its moderate corrosion resistance and excellent mechanical properties [3].

Titanium nitride is a refractory compound distinguished by its high microhardness as well as excellent chemical and thermal stability. TiN serves various applications: including its use in special refractories and cermet, crucibles for anoxic casting of metals, and as a precursor for wear-resistant and to improve surface properties [4, 5]. Due to its inherent biocompatibility, chemical inertness, antibacterial characteristics. favorable tribological properties, TiN coating is considered a suitable material for dental implants [6]. Boron nitride (BN) and BN composite BN is are structural analogs of carbon and occur in the form of sp^2 hybridized hexagonal (h-BN) and rhombohedral (r-BN) or sp^3 bonded quartzite and cubic BN (c-BN) phases [7, 8].

The structure of h-BN can be manufactured into zero-dimensional (0D) fullerene-like structures, one-dimensional (1D) nanotubes, 2D nanosheets, and three-dimensional (3D) bulk crystal structures [9]. The excellent biocompatibility of h-BN has led to its use in several exciting applications, including its use as a drug delivery vector and as an additive in tissue

scaffolds to enhance the thermal and mechanical properties of bio composites [10]. However, the tendency for crack formation at the interface during coating is a significant challenge. Therefore, composite powders of alloys and ceramics are usually prepared to enhance the surface characteristics of the substrate [11].

ISSN: 2073-9524

Pages:57-66

Despite its potential, the available literature on laser-cladded AISI 420 SS coatings remains limited. To enhance the properties of these coatings [12]. MSS coatings with a variety of vanadium (V) contents using a specialty laser cladding technique. The tensile strength and micro-hardness of the target increased firstly and then decreased as the V content increased, while the elongation increased [12].

Li et al. [13] present the martensitic stainless steel (MSS) coatings with niobium (Nb) contents by a laser cladding technique. The addition of Nb was created to significantly improve the corrosion resistance of the laser-cladded MSS coating.

The present work investigates the use of MSS, particularly AISI 420, in applications that require high micro-hardness, good wear resistance, and excellent bio-corrosion. This type of steel is well-suited for a wide range of engineering and medical instruments, including scalpels, surgical blades, forceps and scissors.

2. Materials and Methods

Commercially available cladding material is a titanium nitride powder whose particle size was >3 μm and was procured from Sigma Aldrich. A fine White powder of boron nitride was provided by Sky Spring nanomaterials company, which Particle Size of powder approximately ~ 3 micron with Purity: 99.99%, Plate 420 stainless steel, of 2 \times 20 \times 60 mm, dimensions are used as the substrate. The compositions of the 420-steel substrate are given in Table 1.

Table 1: Chemical Compositions of the base or substrate (wt. %).

Alloying Elements	С%	Si%	Mn%	P%	S%	Cr%	Mo%	Ni%	Al%	Cu%	Fe%
%	0.450	0.47	1.188	0.0223	< 0.001	13.67	0.736	0.296	< 0.001	0.0967	Bal.

2.1 Laser cladding process

Before the experiment, the surface of the sample was polished by metallographic sandpaper to

remove the oxide film on the surface and enhance the bonding strength between the coating and substrate, and then washed with alcohol. The tests were performed using a fiber laser (CW fiber laser-1500W, China). The laser processing conditions were selected: the laser power 1–100-watt, spot size 0.6 mm pulse width 81 nanosecond, the frequency 20-80 KHz, and wavelength 1064 nm. Table 2 shows the parameter settings of the study work.

Table 2: Process parameters of the present work.

	Conditions	
	High power	Low power
Power (watt)	50	30
Frequency (KHz)	25	25
Hatch (mm)	0.005	0.009
Scan speed (mm/s)	1	1
Distance off (cm)	12	12

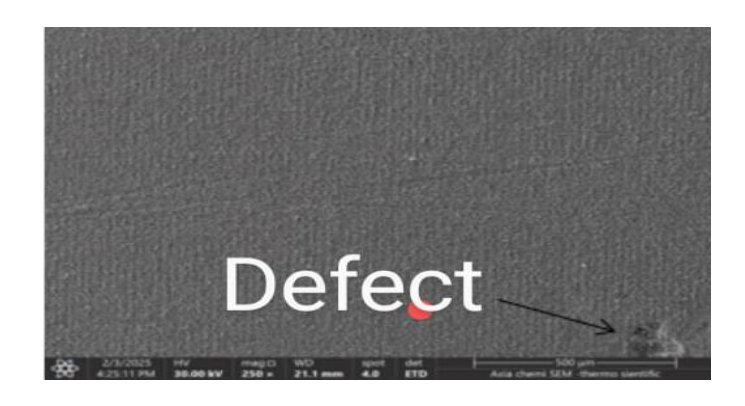
3. Results and Discussion

3.1 SEM (scanning electron microscopy) Microstructure Analysis

The SEM morphology of the region formed between the substrate and the stainless-steel laser clad layer at various powers have good metallurgical bonding between the coated layer and the substrate. Spraying the sample with gold prevents the charging effect on the sample, especially if the TiN is insufficiently conductive. Improves image quality and reduces noise in SEM.

1. Mixture [high power]

Fig. 1 The surface exhibited a uniform and textured appearance, characterized by fine grains. The distribution of the TiN and BN mixture across the steel surface was relatively homogeneous. However, the lower-right area of Fig. 1 displayed a larger dark spot that appeared rougher than the surrounding surface. This was likely a localized defect caused by a slight accumulation of material or interference from the laser beam at that specific point.



ISSN: 2073-9524

Pages:57-66

Fig. 1 SEM morphologies of cross-sections of the (TiN and BN) cladding

In Fig. 2, the surface was composed of very fine and highly homogeneous grains. The visible granules were likely TiN crystals, known for their solid cubic structure. BN molecules were probably distributed either between or within these granules. No visible cracks, pores, or gaps were observed, indicating excellent cohesion between the composite powder and the base material. The coating appeared both homogeneous and dense, reflecting complete coverage of the steel surface.

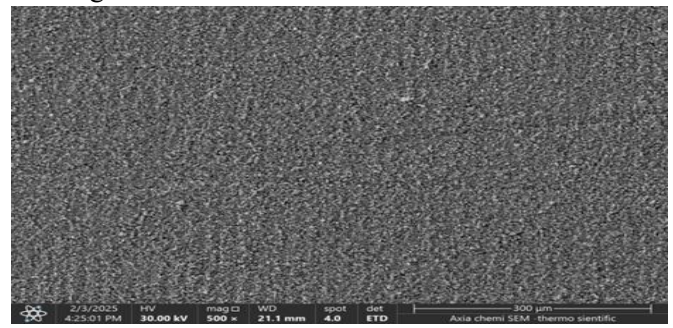


Fig. 2 Cross-sectional SEM image of the (TiN and BN) cladding

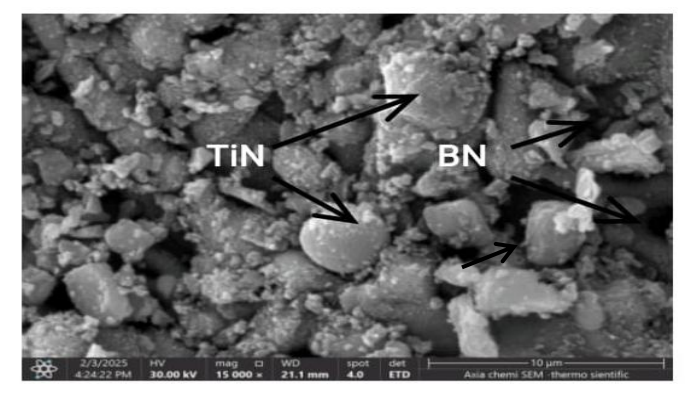


Fig. 3 Cross-sectional SEM image of the (TiN and BN) cladding

Fig. 3 shows the visible particles exhibited irregular shapes and consisted of a mixture of spherical and semi-spherical grains, as well as some

angular particles. Agglomeration was clearly observed. The larger particles were expected to be composed of titanium nitride (TiN) due to its high density, while the smaller or encapsulated particles were likely boron nitride (BN), known for its lubricating and porous properties. The uniform distribution of granules indicated that the coating process was successful in integrating and evenly distributing the materials.

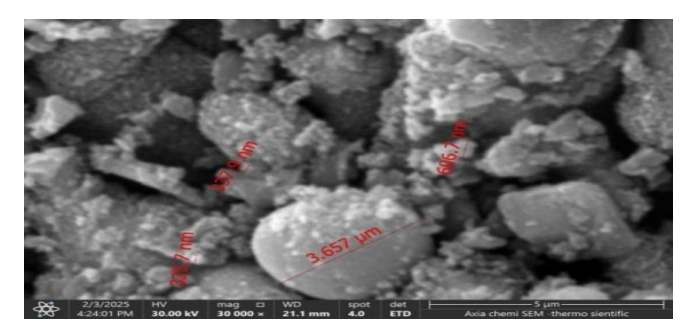
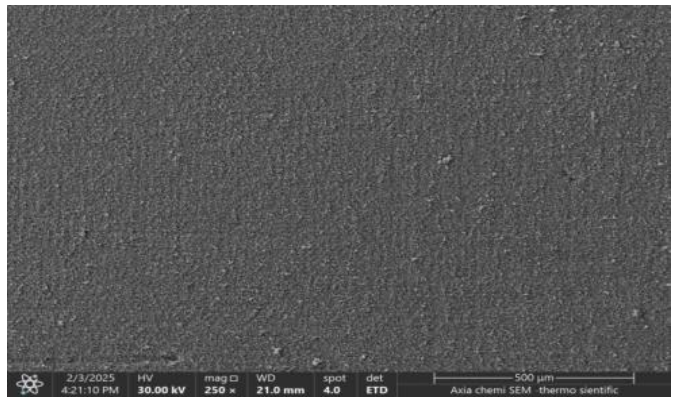


Fig. 4 Cross-sectional SEM image of the (TiN and BN) cladding

Fig. 4 displays irregular masses of particles with crystals of various shapes. The largest particle measured 3.657 µm. Nuclei for the growth of new phases of TiN or BN may have formed around these particles. Typically, these new phases developed into solid and well-defined crystal structures (appearing light gray in SEM Figs). BN was observed as smooth layers or granules, mostly appearing in dark gray. These materials were not only visually distinguishable using SEM, but their varying shapes and sizes also suggested a heterogeneous distribution of the two materials within the coated layer.

2. Mixture (low power)

In Fig. 5, the surface appeared uniform and free of cracks or large gaps. No significant lumps or burrs were observed, indicating that the painting process had been consistent and smooth. This visual quality suggested a strong bond between the paint and the base metal, with a fine distribution of granules.



ISSN: 2073-9524

Pages:57-66

Fig. 5 Cross-sectional SEM image of the (TiN and BN) cladding

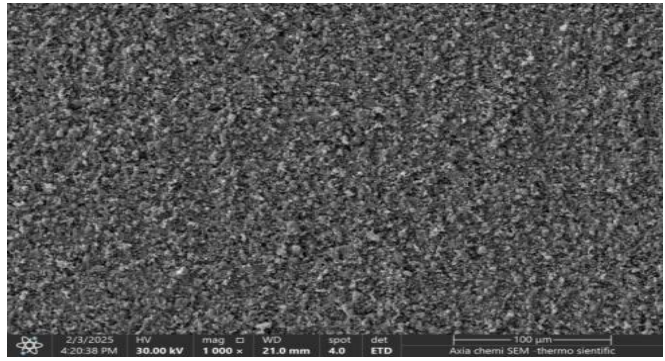


Fig. 6 Cross-sectional SEM image of the (TiN and BN) cladding

Fig. 6 illustrates a microstructure with a controlled granular distribution. The presence of light and dark areas indicated variations in chemical composition, with the lighter regions likely rich in solid compounds such as titanium nitride (TiN) and boron nitride (BN). The presence of very small grains may have suggested the formation of a homogeneous phase resulting from reactions between nitrides and iron within the steel matrix.

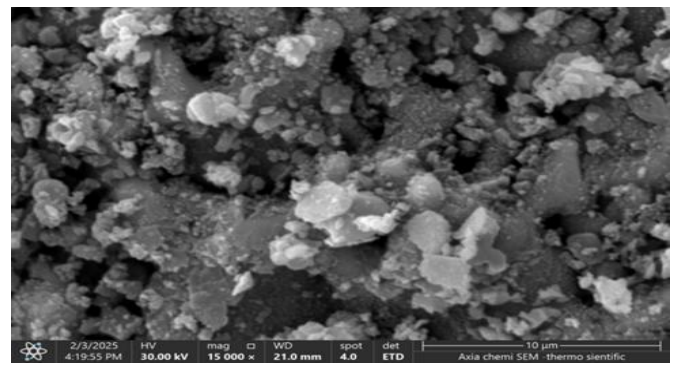


Fig. 7 Cross-sectional SEM image of the (TiN and BN) cladding

Fig. 7 presents the structure, which appears relatively homogeneous, with distinct particles of varying sizes, indicating a well-distributed elemental

composition. The image demonstrated a clear and accurate distribution of TiN and BN compounds across the steel surface following the laser cladding process. In this heterogeneous surface, titanium nitride (TiN) was observed as diffuse solid particles within the nanostructure and micron-sized domains, while boron nitride (BN) appeared as smaller, finer granules. This distribution suggested a successful integration of both materials at different scales.

Fig. 8 confirmed the effectiveness of the laser cladding process in combining TiN and BN on the steel substrate. The observed variation in particle size reflected an irregular yet purposeful distribution aimed at enhancing the surface properties. Titanium nitride (TiN) appeared as brighter regions, consistent with its high hardness and excellent corrosion resistance

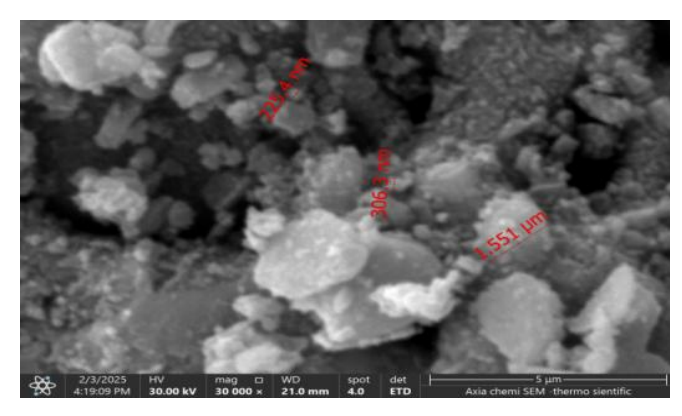


Fig. 8 Cross-sectional SEM image of the (TiN and BN) cladding

3.2 EDS (energy dispersive spectroscopy)

SEM attached to an energy dispersive X-ray analyzer (EDS) was carried out to analyze the unetched clad layer. The comparative analysis of EDX is displayed in Fig. 9, whereas the first sample exhibited a lower Fe (iron) intensity, indicating a thicker or more effective coating layer that limited the detection of the underlying substrate

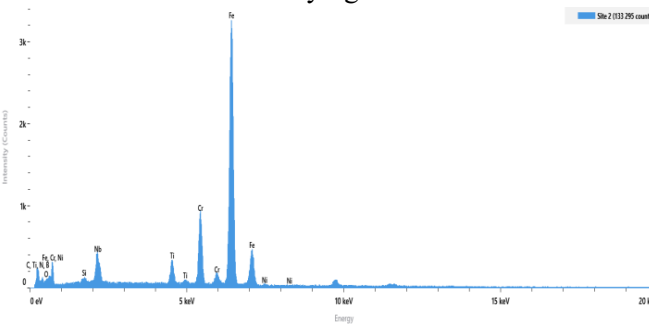


Fig. 9 illustrates EDS analysis of titanium nitride on the sample at higher power.

ISSN: 2073-9524

Pages:57-66

In contrast, the second sample showed in Fig. 10 very high Fe peaks, suggesting that the EDX analysis detected a substantial portion of the base material, which implied a thinner coating or less uniform coverage.

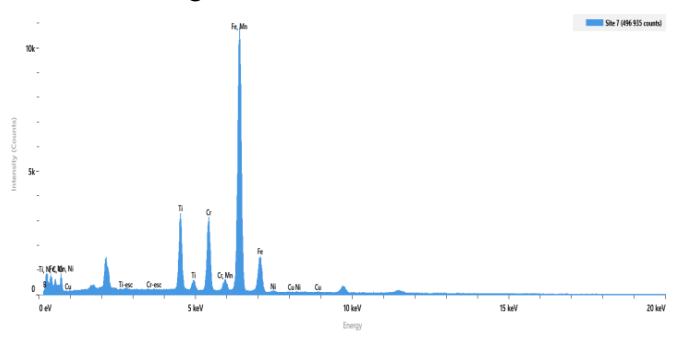


Fig. 10 illustrates the EDS Analysis of Titanium Nitride on the Sample Low Power.

Comparative Analysis of EDX The first sample exhibited a lower Fe (iron) intensity, indicating a thicker or more effective coating layer that limited the detection of the underlying substrate. In contrast, the second sample showed very high Fe peaks, suggesting that the EDX analysis detected a substantial portion of the base material, which implied a thinner coating or less uniform coverage. From a surface engineering perspective, the highpower sample was deemed superior due to its lower Fe signal, which implied improved coating thickness or surface coverage. Additionally, it displayed a cleaner spectrum with fewer impurities, reflecting more uniform deposition and consistent process control. The effective presence of TiN and BN components further supported the quality of the coating. On the other hand, although the low-power sample demonstrated the presence of Ti and BN, the stronger Fe signal indicated a thinner coating with greater substrate influence, potentially reducing its protective performance and durability.

There was no true chemical mixing between titanium nitride (TiN) and boron nitride (BN) to form a secondary compound with a homogeneous phase. Each retained its unique crystal structure, along with its distinct physical and chemical properties. However, during the laser cladding process, TiN and BN were uniformly distributed on the surface of the steel. This enabled the material to

benefit from a combination of desirable properties: the high hardness imparted by TiN and the wear and friction resistance provided by BN. Although a direct chemical reaction or the formation of a new joint phase was unlikely, the uniform distribution within the clad layer significantly enhanced the surface performance of the steel by effectively combining its advantages without any atomic-level mixing.

3.3 Microhardness Test

The average hardness values HV were presented in Tables 3 and 4. The base substrate exhibited a hardness of 208.5 HV. Specimens coated with a TiN/BN (mixture) layer in combination with a thin Ti layer generally showed higher hardness values. Among all tested specimens, those subjected to low-power laser treatment demonstrated the highest hardness. Overall, increased hardness in the specimens was likely to reduce wear loss; however, it was noted that higher hardness did not always correspond to lower wear loss.

Table 3: The microhardness and wear rate results at lower power laser gladding

lower power laser gladding					
Specimen	Micro-hardness (HV)	Wear rate $\times 10^{-3}$ $(mm^3/ \text{ N} \cdot \text{m})$			
A	245.0	0.836			
В	219.9	1.243			
С	261.4	0.465			
D	237.1	0.915			
E	256.8	0.681			

A clear difference in hardness was noticed between the two targets. The high-power sample recorded a Vickers hardness of 191.9 HV, whereas the low-power sample exhibited a higher value of 245.0 HV. Fig. 11 shows the high-power sample recorded a Vickers hardness of 191.9 HV.

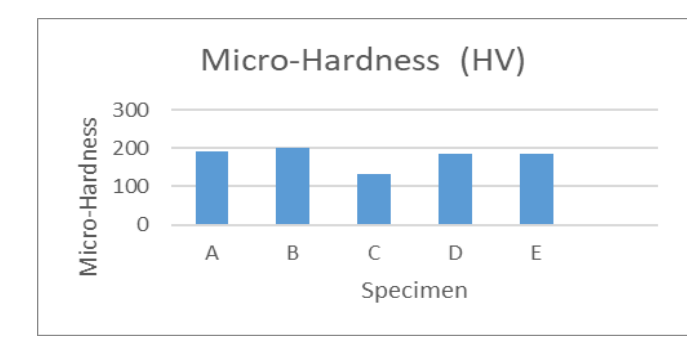


Fig. 11 The microhardness of the as-obtained specimens [higher power].

ISSN: 2073-9524

Pages:57-66

Table 4: The microhardness and wear rate results at high power laser gladding

Specimen	Micro-hardness (HV)	Wear rate $\times 10^{-3}$ $(mm^3/ \text{ N} \cdot \text{m})$
A	191.9	0.138
В	200.3	0.105
С	133.0	0.438
D	185.5	0.260
E	184.6	0.252

3.4 Wear Test

The wear tests were conducted using a specimen wear-testing machine equipped. All targets were subjected to the same load of 222.4 N, and the sliding motion continued until a distance of 2023 m was reached. The wear performance of both samples was assessed through standard tribological testing, and the results showed that sample (high power) had a significantly lower wear rate compared to sample (low power). Specifically, the sample (first) had a wear rate of $0.138 \times 10^{-3} \text{mm}^3/\text{N} \cdot \text{m}$, while the sample (second) recorded a higher rate of 0.836×10⁻³ mm³/N·m, indicating its superior wear resistance. This enhanced property can be attributed to the sample's (low power)'s higher hardness and more compact microstructure. As a result, the sample (low power) is better suited for applications that involve sustained mechanical contact and frictional stress, as shown in Fig. 12 and Fig. 14.

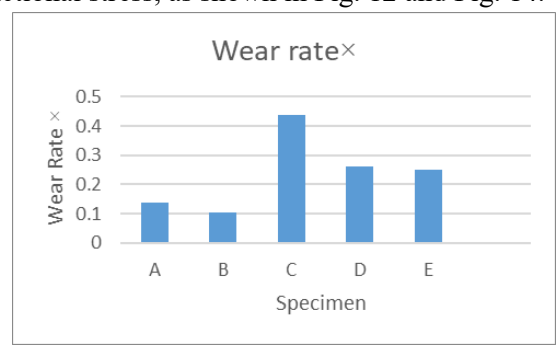


Fig. 12 The wear rate of the as-obtained specimens [higher power].

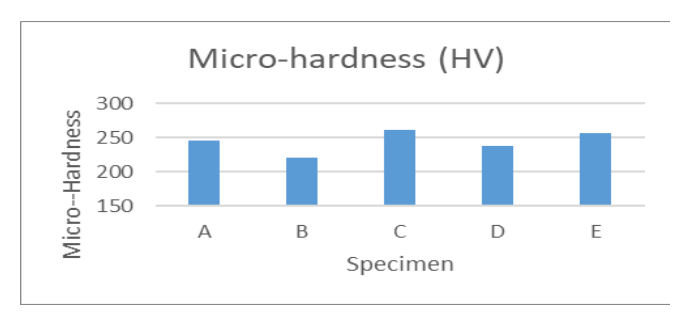


Fig. 13 The microhardness of the as-obtained specimens [lower power].

Whereas Fig. 13 shows the low-power sample exhibited a higher value of 245.0 HV. This increased hardness was particularly advantageous in applications requiring enhanced surface durability and mechanical integrity. The superior hardness of the low-power sample indicated a more refined and densely packed microstructure, which contributed to improved resistance to plastic deformation under mechanical loading.

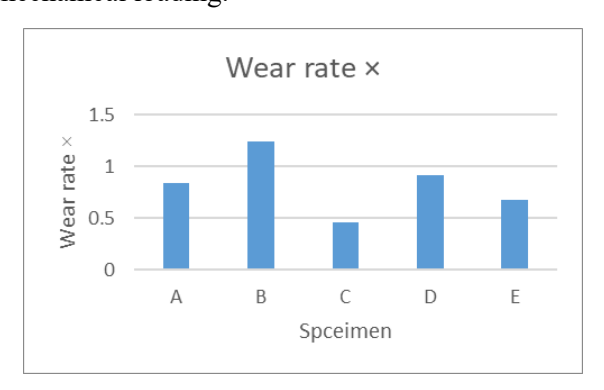
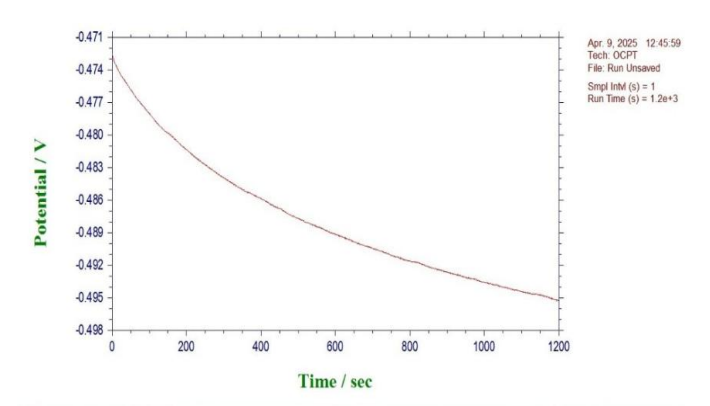


Fig. 14. The wear rate of the as-obtained specimens [lower power].

3.5 Bio-corrosion resistance test.

Purpose of the OCP: Measuring the open voltage of the circuit over time helps assess the stability of the metal surface and its electrochemical activity when exposed to a bio-environment (such as body fluids or solutions containing chloride). The SBF was prepared following the modified Kokubo protocol, which replicates the ion concentrations found in human blood plasma. The composition of the solution. The test was conducted at a temperature of 37 ± 1 °C to simulate physiological conditions and lasted for a duration of 7 days. When compared to the uncoated sample in Fig. 15.



ISSN: 2073-9524

Pages:57-66

Fig. 15 illustrates a bio-corrosion test using Open Circuit Potential (OCP) technology for the base substrate (martensitic stainless steel).

The double-layer TiN+BN coating produced through laser cladding, as shown in Fig. 16, significantly enhanced the bio-corrosion resistance of martensitic steel.

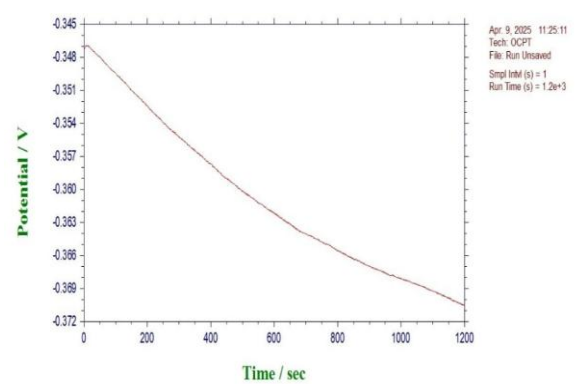


Fig. 16 illustrates bio- corrosion test using Open Circuit Potential (OCP) technology mixture clad layer [TiN +BN].

When compared to the uncoated sample, the double-layer TiN+BN coating produced through laser cladding significantly enhanced the biocorrosion resistance of martensitic steel. This improvement in surface characteristics made the material more suitable for biomedical applications, such as orthopedic implants, dental tools, or surgical instruments.

In contrast, the uncoated martensitic steel demonstrated a more negative and unstable Open Circuit Potential (OCP) profile, reflecting higher electrochemical activity and increased vulnerability to corrosion in a biological environment. Conversely, the TiN+BN coated sample exhibited a less negative and more stable OCP response, signifying improved corrosion resistance. This enhancement was attributed to the ceramic nature of the TiN and BN layers, which offered both chemical

and physical protection. Additionally, the laser cladding process facilitated the formation of a dense and adherent coating, minimizing microstructural defects and further improving bio-corrosion performance.

3.6 Electrochemical analysis

In this context, martensitic steel in Fig. 17 exhibited considerable corrosive activity in a biological medium, as indicated by the current values at the corrosion potential (Ecorr). These results are in the Figs. 18, 19, and 20 provided valuable insights into the electrochemical stability of the material and facilitated comparisons between different materials or the same material before and after surface treatments.

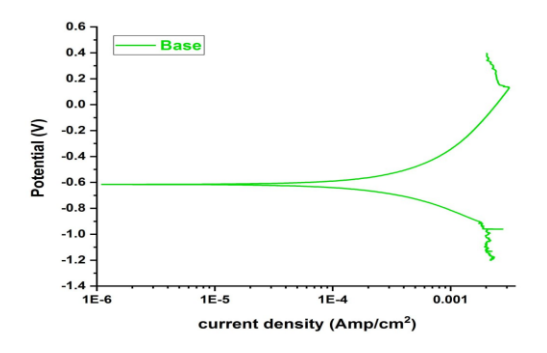


Fig. 17 illustrates Electrochemical Testing for base substrate (martensitic stainless steel) (Potentiodynamic Polarization Curve)

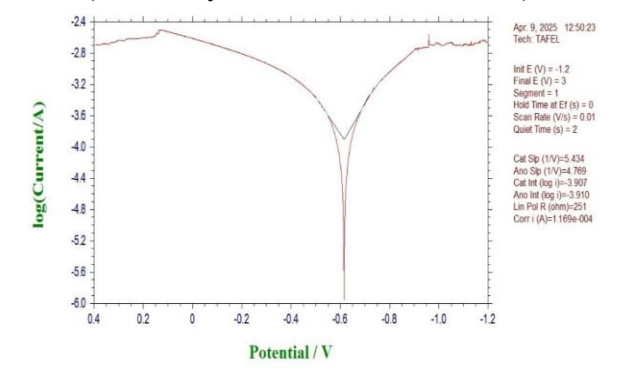
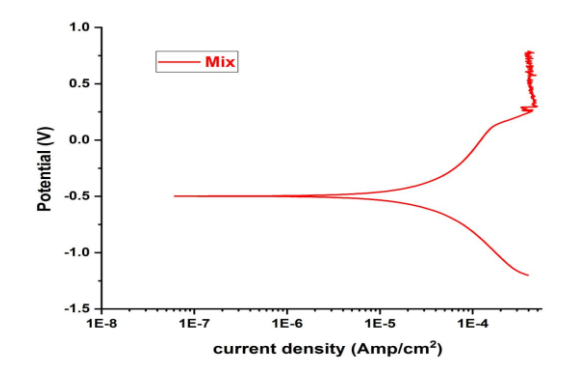


Fig. 18 illustrates Electrochemical Testing for base substrate (martensitic stainless steel) Tafel Plot



ISSN: 2073-9524

Pages:57-66

Fig. 19 illustrates Electrochemical Testing for cladded layer: (a) (Potentiodynamic Polarization Curve)

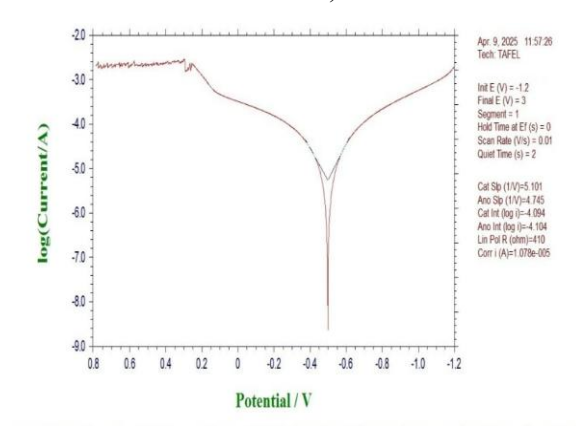


Fig. 20 illustrates the Electrochemical Testing for the cladded layer Tafel Plot.

4. Conclusion

In this study, the following points can be drawn.

- In the (SEM) analysis, microhardness and the adhesion of the coating layer to the substrate material showed that the sample of low power was found to have demonstrated superior microstructural characteristics compared to the Sample high power. The micrographs of the Sample's low power revealed a more homogeneous coating, with fewer microcracks and improved interfacial bonding with the substrate. This was interpreted as indicating stronger and more uniform adhesion across the coated surface.
- The low-power sample exhibited the highest microhardness value, resulting in an increased hardness of the steel compared to the high power sample.
- The EDS showed Sample of high power is superior due to Lower iron (Fe) signal, Sample

low power despite showing strong Ti and BN components. although the low-power sample demonstrated the presence of Ti and BN, the stronger Fe signal indicated a thinner coating with greater substrate influence, potentially reducing its protective performance and durability.

- The high -power sample exhibited the highest wear rate compared to the low -power sample. This result highlights the advantage of selecting the low -power sample for its superior wear resistance.
- The bio-corrosion resistance test demonstrated that the coated sample exhibited significantly better corrosion resistance compared to the uncoated stainless-steel substrate. During the testing period, the coated surface showed minimal signs of degradation, with no evidence of localized corrosion
- The electrochemical techniques result in the "Mix" sample showing superior electrochemical performance compared to the "Base" sample. It had a broader current density range, higher current response, and clearer anodic/cathodic separation, making it more effective for medical instruments.

The primary objective of the current work was to enhance both the mechanical and biological characteristics of the steel. The results demonstrated a significant increase in microhardness following the treatment, which indicated an improvement in the structure. material's internal Additionally, noticeable enhancement in wear resistance was observed, highlighting the steel's improved ability to withstand surface stresses and friction in harsh environments. Furthermore, the treatment resulted in a reduction in the metal's toxicity, which improved its biocompatibility and made it more suitable for medical and environmental applications. These combined improvements confirmed the treatment's effectiveness in enhancing the performance and sustainability of the steel.

References

[1] Guo, W., Li, X., Ding, N., Liu, G., He, J., Tian, L., ... & Zaïre, F. (2021). Microstructure characteristics and mechanical properties of a

laser cladded Fe-based martensitic stainless-steel coating. Surface and Coatings Technology, 408, 126795. DOI:10.1016/j.surfcoat.2020.126795

ISSN: 2073-9524

Pages:57-66

- [2] Zhu, H., Ouyang, M., Hu, J., Zhang, J., & Qiu, C. (2021). Design and development of TiCreinforced 410 martensitic stainless-steel coatings fabricated by laser cladding. Ceramics International, 47(9), 12505-12513. DOI:10.1016/j.ceramint.2021.01.108
- [3] Zhu, H., Li, Y., Li, B., Zhang, Z., & Qiu, C. (2018). Effects of low-temperature tempering on microstructure and properties of the laser-cladded AISI 420 martensitic stainless-steel coating. Coatings, 8(12), 451. DOI:10.3390/coatings8120451
- [4] Prokudina, V. K. (2017). Titanium nitride. In Concise encyclopedia of self-propagating hightemperature synthesis (pp. 398-401). Elsevier. DOI: https://doi.org/10.1016/B978-0-12-804173-4.00160-5.
- [5] Geetha, C. S., Sabareeswaran, A., & Mohanan, P. V. (2012). Pre-clinical evaluation of titanium nitride-coated titanium material. Toxicology mechanisms and methods, 22(2), 144-150. DOI:10.3109/15376516.2011.610384.
- [6] Panjan, P., Drnovšek, A., Terek, P., Miletić, A., Čekada, M., & Panjan, M. (2022). Comparative study of tribological behavior of TiN hard coatings deposited by various PVD deposition techniques. Coatings, 12(3), 294. DOI:10.3390/coatings12030294.
- [7] Otitoju, T. A., Okoye, P. U., Chen, G., Li, Y., Okoye, M. O., & Li, S. (2020). Advanced ceramic components: Materials, fabrication, and applications. Journal of industrial and engineering chemistry, 85, 34-65. DOI:10.1016/j.jiec.2020.02.002.
- [8] Chen, Y., Xu, Y., Li, T., Du, J., Guo, L., & Hu, K. (2025). Fabrication and characterization of self-lubricating anti-wear 316L stainless steel/h-BN composite coatings on Q235 substrate via laser cladding. Optics & Laser Technology, 180, 111564. DOI: https://doi.org/10.1016/j.optlastec.2024.111564.
- [9] Suhail, A., & Lahiri, I. (2020). Two-dimensional hexagonal boron nitride and borophenes. Layered 2D Advanced Materials and Their

ISSN: 2073-9524

Pages:57-66

- Allied Applications, 303-336. DOI:10.1002/9781119655190.ch13.
- [10] Roy, S., Zhang, X., Puthirath, A. B., Meiyazhagan, A., Bhattacharyya, S., Rahman, M. M., ... & Ajayan, P. M. (2021). Structure, properties and applications of two-dimensional hexagonal boron nitride. Advanced Materials, 33(44), 2101589. DOI:10.1002/adma.202101589.
- [11] Zhao, Y., Yu, T., Guan, C., Sun, J., & Tan, X. (2019). Microstructure and friction coefficient of ceramic (TiC, TiN and B4C) reinforced Nibased coating by laser cladding. Ceramics International, 45(16), 20824-20836. DOI:10.1016/j.ceramint.2019.07.070.
- [12] Hu, W., Zhu, H., Hu, J., Li, B., & Qiu, C. (2020). Influence of vanadium microalloying on microstructure and property of laser-cladded martensitic stainless-steel coating. Materials, 13(4), 826. DOI:10.3390/ma13040826.
- [13] Li, B. C., Zhu, H. M., Qiu, C. J., & Zhang, D. K. (2020). Development of high strength and ductile martensitic stainless-steel coatings with Nb addition fabricated by laser cladding. Journal of Alloys and Compounds, 832, 154985. DOI: https.